

Expression of *gibberellin 2-oxidase 4* from *Arabidopsis* under the Control of a Senescence-associated Promoter Results in a Dominant Semi-dwarf Plant with Normal Flowering

Dong Hee Lee¹, In Chul Lee², Kook Jin Kim¹, Dong Su Kim¹, Hyung Jin Na¹, In-Jung Lee³, Sang-Mo Kang³, Hyung-Woo Jeon⁴, Phi Yen Le⁴ and Jae-Heung Ko^{4*}

¹Genomine Advanced Biotechnology Research Institute, Genomine, Inc., Pohang 790-834, Korea

²Department of New Biology, DGIST, Daegu 711-873, Korea

³School of Applied Biosciences, Kyungpook National University, Daegu 702-701, Korea

⁴Department of Plant & Environmental New Resources, Kyung Hee University, Yongin 446-701, Korea

Received: December 16, 2013 / Accepted: January 3, 2014

© Korean Society of Plant Biologists 2014

Abstract Gibberellin (GA), a plant hormone, is involved in many aspects of plant growth and development both in vegetative and reproductive phases. GA2-oxidase plays a key role in the GA catabolic pathway to reduce bioactive GAs. We produced transgenic *Arabidopsis* plants expressing GA2-oxidase 4 (*AtGA2ox4*) under the control of a senescence-associated promoter (*SEN1*). As we hypothesized, transgenic plants (*SEN1::AtGA2ox4*) exhibited a dominant semi-dwarf phenotype with a decrease of bioactive GAs (e.g., GA4 and GA1) up to two-fold compared to control plants. Application of bioactive GA3 resulted in increased shoot length, indicating that the GA signaling pathway functions normally in the *SEN1::AtGA2ox4* plants. Expressions of other members of GA2-oxidase family, such as *AtGA2ox1*, *AtGA2ox3*, *AtGA2ox6*, and *AtGA2ox8*, were decreased slightly in the flower and silique tissues while GA biosynthetic genes (e.g., *AtGA20ox1*, *AtGA20ox2* and *AtGA3ox1*) were not significantly changed in the *SEN1::AtGA2ox4* plants. Using proteome profiling (2-D PAGE followed by MALDI-TOF/MS), we identified 29 protein spots that were increased in the *SEN1::AtGA2ox4* plants, but were decreased to wild-type levels by GA3 treatment. The majority were found to be involved in photosynthesis and carbon/energy metabolism. Unlike the previous constitutive over-expression of GA2-oxidases, which frequently led to floral deformity and/or loss of fertility, the *SEN1::AtGA2ox4* plants retained normal floral morphology and seed production. Accordingly, the expressions of FT and CO genes remained unchanged in the

SEN1::AtGA2ox4 plants. Taken together, our results suggest that the dominant dwarf trait carried by *SEN1::AtGA2ox4* plants can be used as an efficient dwarfing tool in plant biotechnological applications.

Keywords: *Arabidopsis*, Dwarf, Flowering, Gibberellin, Gibberellin 2-oxidase, Senescence-associated promoter

Introduction

Gibberellin (GA) is an essential hormone that is involved in many aspects of plant growth and development in both vegetative and reproductive phases, such as germination, stem elongation, leaf expansion, flower initiation and fruit development (Harberd et al. 1998; Fleet and Sun 2005; Hedden and Thomas 2012). The GA biosynthetic pathway has long been studied, and most of genes encoding enzymes in biosynthetic and catabolic pathways have been identified and characterized in many plant species including *Arabidopsis* (Olszewski et al. 2002; Hedden and Thomas 2012).

Over one hundred GAs have been found in plants, among which GA1 and GA4 are known as major bioactive GAs. In higher plants, the flux of bioactive GAs is regulated by the balance between their rates of biosynthesis and deactivation. There are three kinds of enzymes, such as gibberellin 20-oxidase (GA20ox), gibberellin 3-oxidase (GA3ox), and gibberellin 2-oxidase (GA2ox). Among them, GA2ox functions to catabolize bioactive GAs (GA1 and GA4) and their immediate precursors (GA9, GA12, GA20 and GA53) to inactive GAs by 2 β -hydroxylation, while GA20ox and

*Corresponding author; Jae-Heung Ko
Tel : +82-31-201-3863
E-mail : jhko@khu.ac.kr

GA3ox synthesize bioactive GAs (Yamaguchi 2008; Hedden and Thomas 2012). Since 2 β -hydroxylated GAs are found in most plant species, 2-oxidation pathway has been suggested to be a major mechanism for GA inactivation (Thomas et al. 1999; MacMillan 2001; Rieu et al. 2008a). The Arabidopsis genome encodes a total of seven GA 2-oxidases belonging to class I (AtGA2ox1, AtGA2ox2, and AtGA2ox3), class II (AtGA2ox4 and AtGA2ox6) and class III (AtGA2ox7 and AtGA2ox8). Members of class I and II have been shown to act as C19-GA 2-oxidases, while class III act on C20-GA (Thomas et al. 1999; Jasinski et al. 2005; Rieu et al. 2008a).

Functional characterizations of *GA2ox* genes have been performed in various plant species (Lester et al. 1999; Martin et al. 1999; Hedden and Phillips 2000; Sakamoto et al. 2001; Busov et al. 2003; Solfanelli et al. 2005; Radi et al. 2006; Appleford et al. 2007; Dijkstra et al. 2008; Rieu et al. 2008a). All of the *GA2ox* that have been studied reduce the levels of bioactive GAs in plants. Thus, overexpression of *GA2ox* induces dwarfism (Sakamoto et al. 2001; Busov et al. 2003; Appleford et al. 2007; Dijkstra et al. 2008; Zhou et al. 2011). On the other hand, the suppression of *GA2ox* expression (e.g., mutation of a pea *PsGA2ox1* and Arabidopsis *GA2ox* quintuple mutant) results in tall and slender phenotypes (Martin et al. 1999; Rieu et al. 2008a).

Dwarfism or semi-dwarfism is one of the most important traits in ornamental plants for pot or garden uses as well as in crop plants and fruit trees for numerous horticultural advantages (Busov et al. 2003; Otani et al. 2013). However, ectopic expressions of *GA2ox* genes induce dwarfism, but are frequently accompanied by undesirable phenotypes, such as delayed flowering time, changes of floral morphologies and/or loss of fertility (Singh et al. 2002). In rice, the expression of the *GA2ox* gene using a constitutive promoter results in dwarfing and loss of fertility (Sakamoto et al. 2001; 2003). Thus, alternative approaches, such as tissue or stage specific expression of *GA2ox* may be useful for producing mildly dwarfed plants with normal fertility (Sakamoto et al. 2003).

In the present study, we produced and characterized transgenic Arabidopsis plants expressing the *AtGA2ox4* gene under the control of a senescence-inducible promoter (*SEN1*). *SEN1* promoter was isolated from a senescence-associated gene of Arabidopsis, *sen1*. Expression of the *sen1* gene was shown to be distinctively regulated by several senescence-inducing factors, such as aging, darkness, sugar starvation, and ethylene or ABA treatment (Oh et al. 1996). The promoter region of *sen1* (designated as *SEN1*) fused to the GUS reporter gene was introduced to tobacco plants, which confirmed its senescence-associated expression (Chung et al. 1997). Further analysis suggested that *SEN1* is induced by the recognition of sugar starvation as a senescence signal

(Chung et al. 1997). Thus, we used *SEN1* promoter to examine the feasibility of using *GA2ox* expression under the control of inducible promoter to restrict the growth of target plant species without compromising flowering. The transgenic plants produced using the *SEN1* promoter in this study exhibit dominant semi-dwarf phenotypes with normal floral morphology and seed production. Our results indicate the possibility of molecular breeding for the modulation of plant architecture without compromising flowering or fruit development by genetically engineering the GA metabolic pathway.

Results

SEN1::AtGA2ox4 Plants Produce a Dominant Semi-dwarf Phenotype

AtGA2ox4 (At1g47990) has been shown to act exclusively as a C19-GA 2-oxidase (Jasinski et al. 2005). As a first step toward *in vivo* functional characterization of *AtGA2ox4*, we generated transgenic Arabidopsis plants expressing a full-length cDNA of *AtGA2ox4* under the control of a senescence-associated promoter (*SEN1*) (i.e., *SEN1::AtGA2ox4* plants). The *SEN1* promoter is induced during senescence, and triggered by stimuli such as aging, darkness, sugar starvation, and ethylene or ABA treatment (Oh et al. 1996; Chung et al. 1997). Twenty-five of the 35 T₁ transgenic plants produced exhibited dwarf phenotypes. Among them, two independent T₃ homozygous lines (9-1 and 10-2) were selected and used in this study. In 30-d-old *SEN1::AtGA2ox4* plants, *AtGA2ox4* transcripts were highly accumulated in all tissues examined (i.e., flower, root, stem, leaf and siliques) compared to control plants (Fig. 1A). Rosette leaves were small, and inflorescent stem elongation was severely retarded compared to wild-type plants (Fig. 1B, C). In 40-d-old mature plants, *SEN1::AtGA2ox4* plants were about half the size of their wild-type counterpart (Fig. 1D).

Dwarf Phenotypes of *SEN1::AtGA2ox4* Plants were Reversed by GA3 Application

GA3 is a bioactive form of GA that cannot be metabolized by endogenous *GA2ox* (Sakamoto et al. 2001). To test our hypothesis that the *SEN1::AtGA2ox4* plants have low bioactive GA levels due to a high rate of inactivation by *GA2ox*, we sprayed 0.1 mM of GA3 on 12-d-old seedlings once per week. Our results clearly showed that normal stem growth was restored and the leaves also returned to normal color and size (Fig. 1 B, C and D). These results indicate that bioactive GAs are deficient, but the GA signaling pathway functions normally in *SEN1::AtGA2ox4* plants.

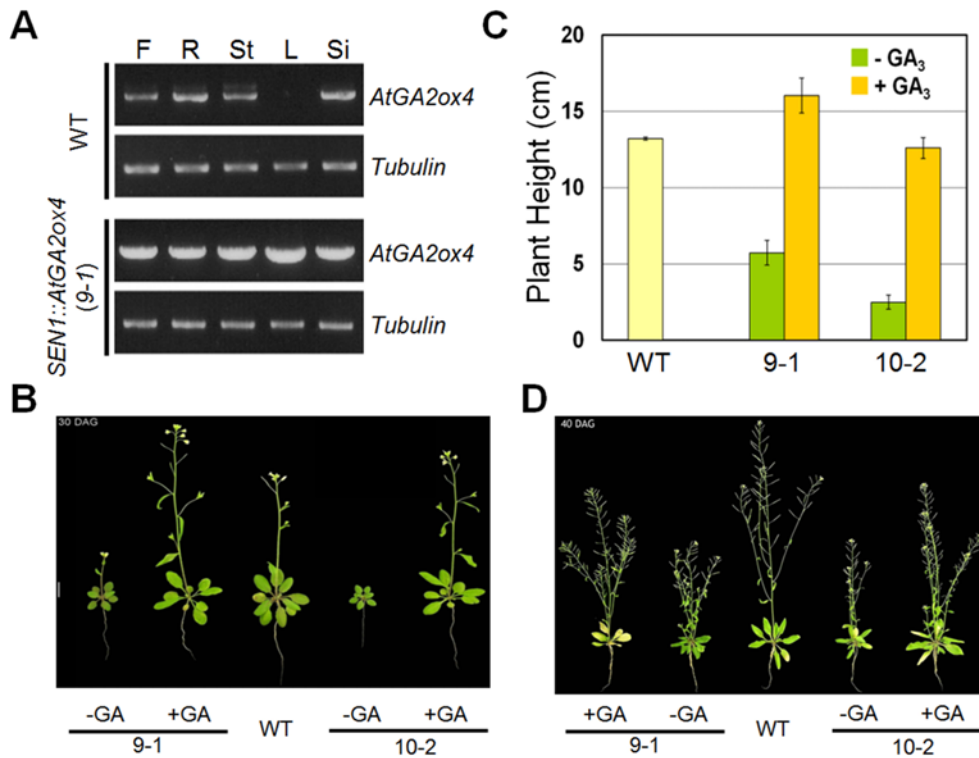


Fig. 1. *SEN1::AtGA2ox4* plants produce a dominant semi-dwarf phenotype, which were reversed by bioactive GA3 application. (A) Tissue specific expression of *AtGA2ox4* and up-regulation of *AtGA2ox4* driven by *SEN1* promoter in transgenic Arabidopsis plant (*SEN1::AtGA2ox4*, line 9-1). (B) Thirty-day-old *SEN1::AtGA2ox4* plants showed a dwarf phenotype (-GA) which was reversed by bioactive GA3 treatment (+GA) compared to wild type plant (WT). Representative pictures of two independent T3 homozygous lines (9-1 and 10-2) were shown. Scale bar indicates 1 cm. (C) Measurement of plant heights of 9-1 and 10-2 lines together with WT. Note that GA3 treatment fully recovered the dwarf phenotype. Error bar means S.E. (n = 10). (D) Forty-day-old *SEN1::AtGA2ox4* plants showed a dwarfing phenotype (-GA) which was reversed by bioactive GA3 treatment (+GA) compared to wild type plant (WT). Representative pictures of two independent T3 homozygous lines (9-1 and 10-2) were shown. Scale bar indicates 1 cm.

SEN1::AtGA2ox4 Plants Have Reduced Levels of Bioactive GAs

To confirm the phenotypic consequences of *SEN1::AtGA2ox4* plants, we measured endogenous GA levels. Both of the independent T3 homozygous lines of the *SEN1::AtGA2ox4* plants (9-1 and 10-2) showed considerably reduced levels of bioactive GA4 and GA1 (up to two-fold decrease), but also exhibited increased levels of the respective inactivation products GA34 and GA8 when compared to wild-type plants (Fig. 2A). These results indicate that the introduced *AtGA2ox4* gene in the *SEN1::AtGA2ox4* plant degraded the endogenous bioactive GAs and resulted in dwarf phenotypes. In addition, we quantified the amounts of various GAs involved in the GA biosynthesis and deactivation pathway starting from GA12 (Fig. 2B). Among them, GA9, GA19, GA24, and GA53, which are immediate precursors of bioactive GA4 and GA1, were slightly increased (Fig. 2A). This is interesting, because GA2ox functions to metabolize not only bioactive GAs (GA1 and GA4), but also their immediate precursors (GA9, GA12, GA20 and GA53) to inactive GAs by

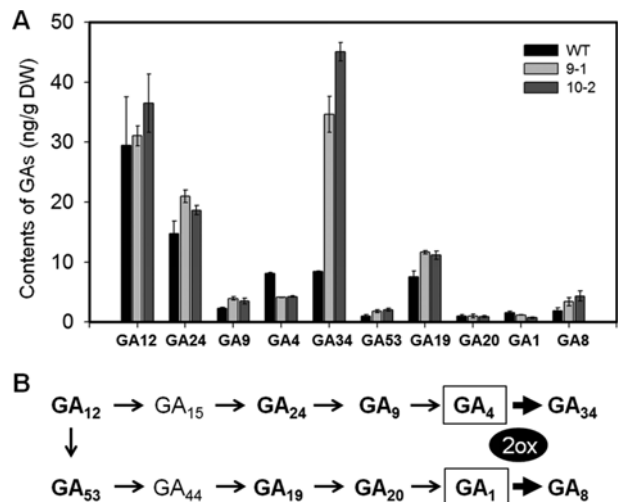


Fig. 2. *SEN1::AtGA2ox4* plants have reduced levels of bioactive GAs. (A) Endogenous contents of various GAs were measured. Error bar means S.D. of three independent experiments. WT, wild type Arabidopsis; 9-1 and 10-2, two independent T3 homozygous lines of *SEN1::AtGA2ox4* plants. (B) GA biosynthesis and deactivation (by GA2ox) pathways from GA12. Measured GAs in A is in bold. GA2ox catabolizes bioactive GAs (GA4 and GA1 in box) to GA34 and GA8.

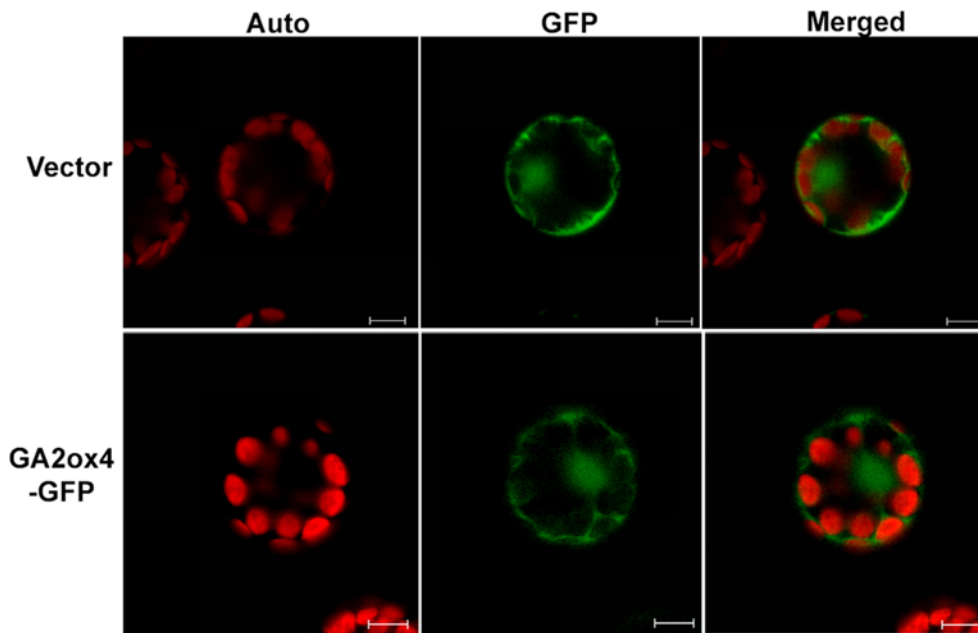


Fig. 3. Subcellular localization of AtGA2ox4. Transient expression of GFP fused AtGA2ox4 under the 35S promoter (GA2ox4-GFP), together with GFP alone (vector) as a control, in Arabidopsis protoplast. GFP fluorescence was visualized using confocal laser scanning microscopy. Auto fluorescence (left panels, ‘Auto’) and GFP fluorescence (center panels, ‘GFP’) images are merged (right panels, ‘Merged’) to illustrate the subcellular localization of the protein. Scale bars indicate 10 μm.

hydroxylating the 2-carbon position, which cannot be reactivated (Thomas et al. 1999; MacMillan 2001).

Subcellular Localization of AtGA2ox4

In our amino acid sequence analysis of various GA2ox, we were unable to identify any known targeting sequences that signify the localization of the protein within the plant cell (data not shown). Since the inactivation of bioactive GAs through GA2ox occurs mainly in the cytoplasm (Hedden and Phillips 2000), we hypothesized that AtGA2ox4 protein may localize in the cytoplasm. To test this hypothesis, we transiently expressed GFP-fused AtGA2ox4 under the 35S promoter (35S::AtGA2ox4:GFP) together with GFP alone (35S::GFP) as a control in Arabidopsis protoplast (Fig. 3). The distribution of GFP fluorescence of AtGA2ox4:GFP was spread throughout the cytoplasm and nucleus, similar to the control. This result suggests that AtGA2ox4 localizes to both the cytoplasm and the nucleus, which is consistent with findings of PslGA2ox from plum (*Prunus salicina* L.) (El-Sharkawy et al. 2012) and OsGA2ox6 from rice (Huang et al. 2010).

Expression of Genes Involved in GA Biosynthesis and Catabolism in SEN1::AtGA2ox4 Plants

To determine the effects of *AtGA2ox4* mis-regulation on expression changes of other members of GA 2-oxidase, we

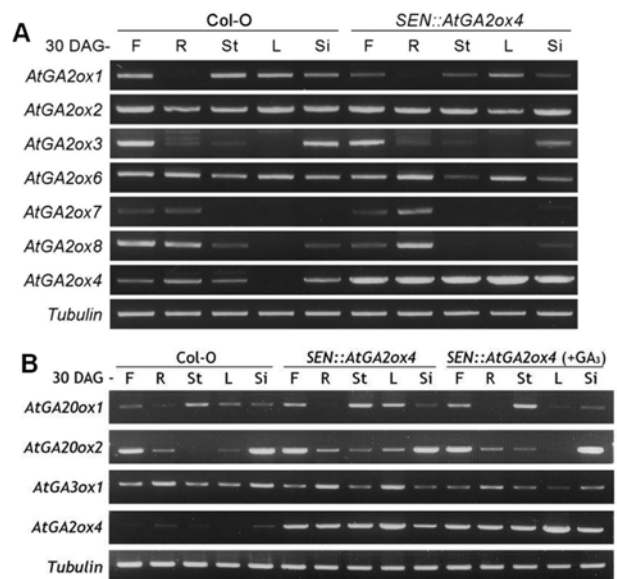


Fig. 4. Expression of genes involved in GA biosynthesis and catabolism in *SEN1::AtGA2ox4* plants. (A) Tissue specific expression patterns of GA catabolizing genes in WT (Col-0) and *SEN1::AtGA2ox4* plants. (B) Tissue specific expression patterns of GA activating genes in WT (Col-0) and *SEN1::AtGA2ox4* plants with (+GA3) or without bioactive GA treatment. Semi-quantitative RT-PCR was performed using 1st cDNAs as templates prepared from tissues of 30 d after germination (DAG) on soil grown plants. F, flowers; R, roots; St, stems; L, rosette leaves; Si, siliques.

analyzed their tissue specific expression profiles using semi-quantitative RT-PCR (Fig. 4A). GA2ox transcripts could be

detected in all tissues analyzed. *AtGA2ox2* and *AtGA2ox6* were the most highly expressed genes in all tissues, and *AtGA2ox1* transcripts reached the highest levels in the flower and stem, which is consistent with the results of Rieu et al (2008a). Interestingly, the expression of *AtGA2ox6* was slightly decreased in the stem and siliques of *SEN1::AtGA2ox4* plants. *AtGA2ox1* transcripts were also decreased in the flower, stem and siliques (Fig. 4A). The expression of *AtGA2ox8* was found mainly in the flower and roots (Fig. 4A). However, expression of *AtGA2ox8* in the flower was significantly decreased in the *SEN1::AtGA2ox4* plants. These results suggest that the mis-expression of *AtGA2ox4* may decrease the gene expressions of other members, especially in the reproductive organs.

On the other hand, the expression of GA biosynthetic genes (e.g., *AtGA20ox1*, *AtGA20ox2* and *AtGA3ox1*) was increased in leaf tissue, but decreased by GA3 treatment in

SEN1::AtGA2ox4 plants (Fig. 4B). A slight increase of *AtGA20ox1* was also detected in flower tissue (Fig. 4B).

Changes of the Proteome in *SEN1::AtGA2ox4* Plants with or Without GA3 Treatment

To characterize GA-related proteome profiling of the *SEN1::AtGA2ox4* plants, we performed 2-D PAGE (two-dimensional polyacrylamide gel electrophoresis) based proteomic analysis. Soluble proteins were obtained from 30-d-old wild type plants, *SEN1::AtGA2ox4* plants, and GA3-treated *SEN1::AtGA2ox4* plants, respectively, and then were separated by 2-D PAGE using isoelectric point (pI) gradient (IPG) strips for the first-dimension separation (pI 4-10) and 12% SDS-PAGE for the second separation. Proteins were visualized with silver staining (Fig. 5). Using PDQuest software (v 7.0, BioRad), we identified 29 protein spots that

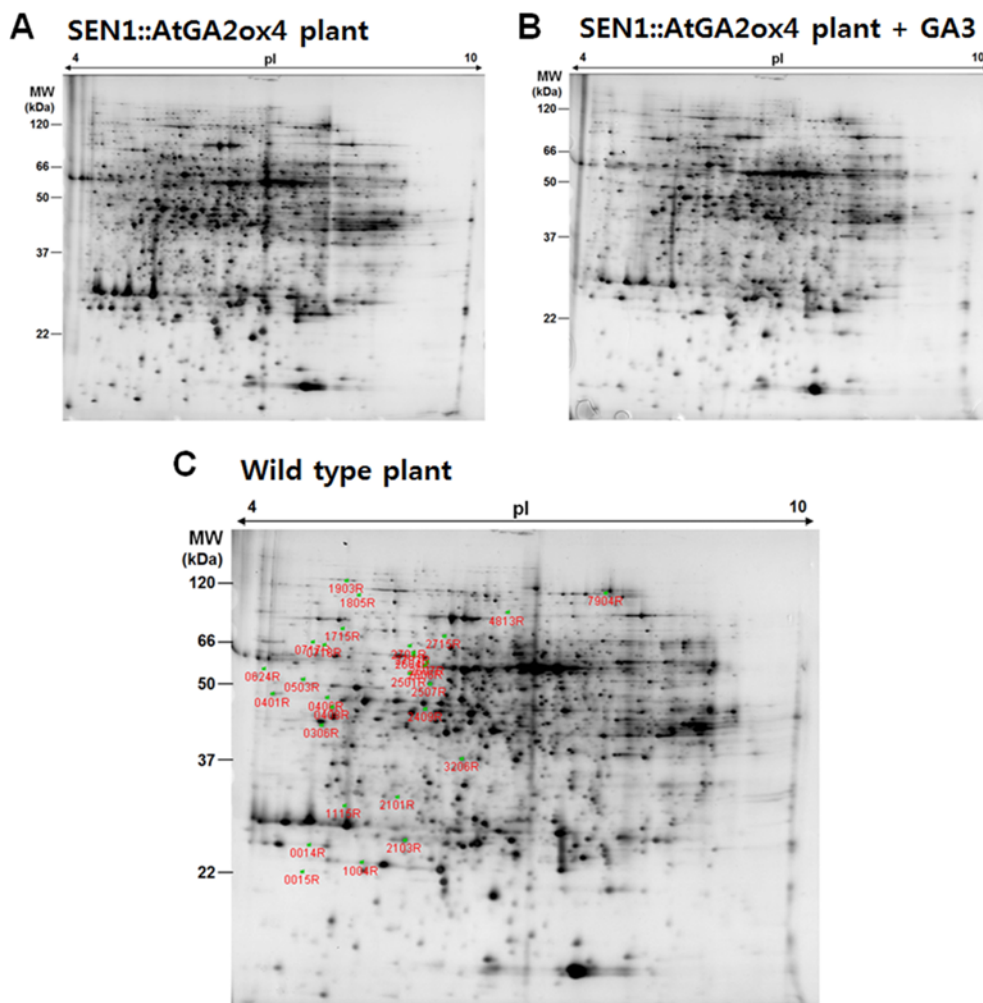


Fig. 5. Changes of proteome in *SEN1::AtGA2ox4* plants with or without GA3 treatment. (A) Two dimensional protein profiles of 30-d-old *SEN1::AtGA2ox4* plants. (B) Two dimensional protein profiles of 30-d-old *SEN1::AtGA2ox4* plants treated with GA3. (C) Two dimensional protein profiles of 30-d-old WT plants. Designated (numbered) spots indicate increased proteins in the *SEN1::AtGA2ox4* plant but decreased to wild type level by GA3 treatment.

Table 1. List of proteins identified from proteomic analysis

Spot I.D.	M.W. (KDa)	AGI	Protein description
14*	25.92	N.D.	LHCB6 (PSII); chlorophyll binding
15	22.3	N.D.	ATP-dependent Clp protease proteolytic subunit
306*	43.09	AT3G55800	SBPASE, sedoheptulose-bisphosphatase
401*	48.75	AT5G30510	RPS1, ribosomal protein S1
406	48.04	AT1G47110	Serpin, serine protease inhibitor
408*	46.25	AT4G18480	CHL11, CHLORINA 42; magnesium chelatase
503	51.78	AT3G05530	26s proteasome AAA-ATPase subunit RPT5a
624*	54.07	N.D.	RuBP carboxylase oxygenase large subunit N-methyltransferase
717	66.33	AT1G25490	RCN1, ROOTS CURL IN NPA; protein phosphatase type 2A regulator
718	64.88	N.D.	Protein phosphatase 2A 65 kDa regulatory subunit
1004*	23.48	N.D.	LHCA4; chlorophyll binding
1115*	31.24	N.D.	LHCP AB 180, chlorophyll a/b binding protein
1715*	73.57	AT4G31390	ABC1-like kinase
1805	96.01	AT3G20630	UBP14, UBIQUITIN-SPECIFIC PROTEASE 14
1903	123.37	AT3G19290	ABF4, ABRE BINDING FACTOR 4
2101*	32.37	N.D.	CA1, CARBONIC ANHYDRASE 1
2103*	26.59	AT5G01600	ATFER1, ferritin 1; ferric iron binding
2409*	45.98	AT5G14200	ATIMD1, Isopropylmalate Dehydrogenase 1
2501*	52.84	N.D.	Gamma-glutamylcystein synthetase
2507*	50.73	AT5G48300	ADG1, ADP Glucose Pyrophosphorylase small subunit 1
2604*	59.62	N.D.	ATP synthase CF1 alpha subunit
2606*	54.92	AT1G17290	ALAAT1, alanine aminotransferase
2701*	64.11	AT1G74920	ALDH10A8, Aldehyde dehydrogenase 10A8
2703*	61.15	AT3G13930	Dihydrolipoamide acetyltransferase
2715*	69.35	AT1G09780	2,3-biphosphoglycerate-independent phosphoglycerate mutase
7904	99.47	AT3G16420	JAL30, JACALIN-related Lectin 30

*, proteins related to photosynthesis and carbon/energy metabolism

were increased in the *SEN1::AtGA2ox4* plants, but were decreased to wild type levels by GA3 treatment. After individual protein spots were selected and in-gel digested with trypsin, protein sequences and genes encoding the proteins were identified by MALDI-TOF/MS (Matrix Assisted Laser Desorption Ionization – Time Of Flight/Mass Spectrometry) analysis coupled with a database search using ProFound (<http://prowl.rockefeller.edu/prowl-cgi/profound.exe>). Protein spots with predicted genes were numbered on the gel as shown in Fig. 5C and listed in Table 1. We identified a total of 26 proteins, which are presumably regulated by *AtGA2ox4* related to GA metabolism. Interestingly, 17 proteins among these were found to be involved in photosynthesis and carbon/energy metabolism (Table 1). In addition, proteins responsive to ABA and JA were also detected (*At3g19290*, *At3g16420*), indicating cross-talk among plant hormones.

SEN1::AtGA2ox4 Plants Exhibited Normal Flowering and Fruit Development

Previously, there were many reports that GA biosynthesis

mutants containing low levels of bioactive GAs showed late flowering, abnormal flower morphologies and/or partial loss of fertility as well as dwarfism (Sun and Kamiya 1994; Silverstone et al. 2001; Schomburg et al. 2003; Rieu et al. 2008a; El-Sharkawy et al. 2012). The flowering time was not different significantly in *SEN1::AtGA2ox4* plants compared to control plants, as measured by counting rosette leaf numbers at the start of bolting (Fig. 6A). However, GA3 applications noticeably reduced flowering time in *SEN1::AtGA2ox4* plants, as expected (Fig. 6A). Tissue specific gene expression patterns of *FT* and *CO*, those are genes controlling flowering time, in *SEN1::AtGA2ox4* plant are very similar to control plants (Fig. 6B). In addition, there were no discernible changes in flower morphologies in the *SEN1::AtGA2ox4* plants (Fig. 6C). However, seed production was significantly enhanced in the *SEN1::AtGA2ox4* plants (Fig. 6C, 6D). The seed morphology of *SEN1::AtGA2ox4* plants is normal and slightly bigger than control's (Fig. 6C). Accordingly, the weight of seeds per plant was much greater in *SEN1::AtGA2ox4* plants (~60 mg) than in control plants (~40 mg) (Fig. 6D). These results suggest that *SEN1::AtGA2ox4* plants exhibit

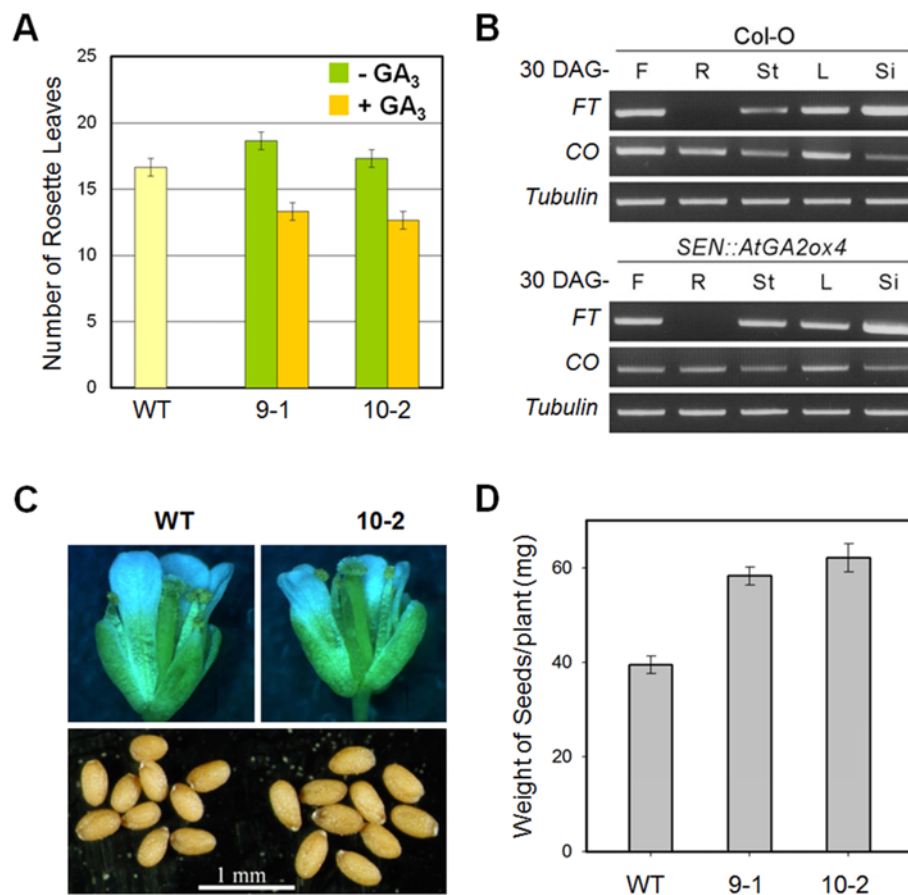


Fig. 6. *SEN1::AtGA2ox4* plants exhibited normal flowering and fruit development. (A) Flowering time measurement by counting number of rosette leaves at bolting. Note that bioactive GA treatment (+GA₃) accelerates flowering of *SEN1::AtGA2ox4* plants. (B) Tissue specific expression of FT and CO genes comparing WT (Col-0) with *SEN1::AtGA2ox4* plants. Semi-quantitative RT-PCR was performed using 1st cDNAs as templates prepared from tissues of 30 d after germination (DAG) on soil grown plants. F, flowers; R, roots; St, stems; L, rosette leaves; Si, siliques. (C) Representative pictures of flower (upper) and seeds (lower) from WT and *SEN1::AtGA2ox4* plant (line 10-2). (D) Weight of seeds harvested from individual plants indicated. Error bars mean S.E. (n = 16).

almost normal flowering capacity without compromising flower morphologies and fruit development.

Discussion

Demands for dwarf plants are increasing, because dwarfism is one of the most important traits in modern agriculture. Plants with reduced stature allow high-density cultivation, facilitate management, minimize spray drift, lessen lodging damage, and increase harvest yield. In this study, we produced a dominant semi-dwarf *Arabidopsis* plant by expression of the *AtGA2ox4* gene under the control of a senescence-associated promoter. Transgenic plants (*SEN1::AtGA2ox4*) exhibited considerable decreases in the levels of bioactive GAs (e.g., GA₄ and GA₁) and increases in the corresponding inactivation products GA₃₄ and GA₈, respectively, in comparison to control plants (Fig. 2). In addition, exogenous treatment of bioactive GA₃ reversed the dwarf phenotypes

of the *SEN1::AtGA2ox4* plants (Fig. 1). These results are consistent with the known function of GA_{2ox}, indicating that the introduced *AtGA2ox4* gene in the *SEN1::AtGA2ox4* plants was functional and resulted in dwarf phenotypes by degrading endogenous bioactive GAs.

Study on the subcellular localization of *AtGA2ox4* suggests that *AtGA2ox4* is localized in both the cytoplasm and nucleus (Fig. 3). This result is consistent with previous reports, such as *PsIGA2ox* from plum (*Prunus salicina* L.) and *OsGA2ox6* from rice (Huang et al. 2010; El-Sharkawy et al. 2012). GA receptors (GID1s) also have similar subcellular localization (Ueguchi-Tanaka et al. 2005). This suggests that coordinate regulation of GA content and signaling might be controlled by GID1s and GA_{2ox}s, which should be further investigated.

To characterize the translation phenotype of the *SEN1::AtGA2ox4* plants regulated by *AtGA2ox4*, we performed two-dimensional protein profiling followed by MALDI-TOF/MS analysis. Among a total of 26 proteins identified, which were

increased in the *SEN1::AtGA2ox4* plant, but decreased back to wild type levels by GA3 treatment (Fig. 5, Table 1), the majority are involved in photosynthesis. The photosynthetic capacity of the whole plant is lower in *AtGA2ox* plants compared to WT, which is correlated with low amounts of dry matter accumulation and the dwarf phenotype. However, unlike *AtGA2ox* plants, *AtGA20ox* plants were tall and exhibited higher photosynthetic capacity than WT (Biemelt et al. 2004). Thus, photosynthesis-associated proteins that were up-regulated in the *SEN1::AtGA2ox4* plants might play compensatory roles to maintain photosynthetic capacity in GA deficient condition.

Very interestingly, the *SEN1::AtGA2ox4* plants retained normal floral morphology and seed production. This result is strikingly unlike those of previous studies of GA deficient mutants or transgenic plants produced by constitutive overexpression of gibberellin 2-oxidases, which frequently led to delayed flowering, floral deformity, and/or loss of fertility (Sun and Kamiya 1994; Silverstone et al. 2001; Singh et al. 2002; Sakamoto et al. 2001, 2003; Schomburg et al. 2003; Radi et al. 2006; Rieu et al. 2008a; El-Sharkawy et al. 2012). This finding may be explained by the senescence-associated promoter driven expression of *AtGA2ox* in the *SEN1::AtGA2ox4* plants. Compared to the constitutive overexpression promoter (e.g., 35S promoter, or actin promoter), the activity of the *SEN1* promoter is associated with leaf senescence. In normal growth conditions, the *sen1* gene is induced in the leaves of 25 d-old plants when inflorescence stems are 2–3 cm high, and the mRNA levels are maintained at similar levels in naturally senescing leaves (Oh et al. 1996). Although high level expression of *AtGA2ox4* was detected in all tissues, including flower and siliques in the 30-d-old *SEN1::AtGA2ox4* plants (Fig. 1A), we hypothesized that no severe changes of bioactive GA levels occurred in the floral organ compared to constitutive overexpression. This hypothesis was supported by the following observations. First, in an analysis of the expressions of genes involved in GA biosynthesis and catabolism in the *SEN1::AtGA2ox4* plants, the expressions of *AtGA2ox1*, *AtGA2ox3* and *AtGA2ox8* were decreased, especially in flower and siliques (Fig. 4A). On the other hand, slight increases of *AtGA20ox1* were observed in flower tissue (Fig. 4B). Thus, reduction of bioactive GAs caused by the higher levels of *AtGA2ox4* in floral organs of the *SEN1::AtGA2ox4* plants may be compensated by the decreased expressions of other *AtGA2oxs* as well as increased expression of *AtGA20ox1*. Second, expression patterns of flowering time-control genes (e.g., *FT* and *CO*) were not changed significantly in the *SEN1::AtGA2ox4* plants compared to control plants (Fig. 6B). Previously, it was found that *FT* expression is regulated by GA levels. For example, GA4 promotes *FT* expression in wild-type (Col-0) plants and is required for *FT* expression in GA deficient mutant, *gal-3* (Col-0) (Hisamatsu

and King 2008; Mutasa-Göttgens and Hedden 2009). Finally, there were no discernible changes in flower morphologies in *SEN1::AtGA2ox4* plants. More interestingly, seed production was significantly enhanced in *SEN1::AtGA2ox4* plants (Fig. 6C, D). The importance of precise control of GA content for the coordinated growth of floral organs is well known (Rieu et al. 2008b). Even mild GA-deficient mutants have impaired male fertility due to abnormal stamen development (Chhun et al. 2007; Hu et al. 2008; Rieu et al. 2008a). Typically, GA-deficient or signaling mutants have shorter stamens than pistils due to reduced cell extension in the filament (Cheng et al. 2004), which results in a partial loss of fertility/reduced seed production from the compromised self-pollination. Taken together, bioactive GA levels in the floral organs of *SEN1::AtGA2ox4* plants were not changed significantly. Enhanced seed production in *SEN1::AtGA2ox4* plants may be the result of allocating energy and carbon resources to producing and filling grains rather than growing taller, as in GA insensitive dwarfing wheat in the Green Revolution (Peng et al. 1999; Hedden 2003). The detailed mechanism should be addressed by further studies.

The aim of the work in this study was to examine the feasibility of using *GA2ox* expression under the control of inducible promoter to restrict the growth of target plant species without compromising flowering and seed production. Our results indicate that *SEN1::AtGA2ox4* plants exhibit almost normal flowering capacity and enhanced seed production as well as a dominant semi-dwarf phenotype, which are valuable traits in plant domestication. Previously, Sakamoto et al. (2003) reported that transgenic rice (*Oryza sativa*) expressing *OsGA2ox1* under the control of the *OsGA3ox2* promoter produced dwarf phenotypes without alterations in floral morphology. Thus, the controlled expression of *GA2ox* through a utility promoter (i.e., an inducible, tissue- or developmental-specific promoter) is an efficient biotechnological tool for producing dwarf or semi-dwarf crops, fruit trees and ornamental plants.

Materials and Methods

Plant materials and Growth Conditions

Arabidopsis thaliana ecotype Columbia (Col-0) was used in both wild-type and transgenic plant experiments. Plants were grown in soil in a growth chamber (16 h light/8 h dark) at 23°C.

RNA extraction and RT-PCR

Total RNAs were extracted using Trizol reagent (Invitrogen, <http://www.invitrogen.com/>) according to the manufacturer's instructions. Five micrograms of total RNA was treated with DNase I and used for first-strand cDNA synthesis using SuperScript II reverse transcriptase (Invitrogen, www.invitrogen.com). RT-PCR was performed using 1 µL of the reaction products as a template.

Amplified DNA fragments were separated on 1% agarose gels and stained with ethidium bromide. The primers used for RTPCR are shown in Table S1.

Plasmid Construction and Plant Transformation

All of the constructs used in this study were verified by DNA sequencing. The full-length cDNA of *AtGA2ox4* (At1g47990) was amplified from Arabidopsis stem cDNA by PCR. The resulting PCR product was subcloned into *Bam*HI and *Bst*EII restriction sites of the pSEN vector, which locates after SEN1 promoter (pSEN; Figure S1). The vector constructs were introduced into *Agrobacterium tumefaciens* strain C58, which was used to transform *Arabidopsis thaliana* (Col-0) by the floral-dip method as described by Clough and Bent (1998). For subcellular localization of AtGA2ox4, a full-length cDNA of *AtGA2ox4* without stop codon was cloned into pMDC84 vector (Curtis and Grossniklaus 2003) to produce AtGA2ox4:GFP fusion protein by using the Gateway cloning method (Invitrogen).

Subcellular Localization of AtGA2ox4

Transfection of Arabidopsis protoplasts with AtGA2ox4:GFP/pMDC84 plasmids was performed as described previously (Ko et al. 2009). Localization of AtGA2ox4:GFP fusion proteins in protoplasts was carried out by confocal scanning laser microscopy (CSLM) on a CSLM 510 Meta (Zeiss, Jena). Excitation was provided by the 458 and 514 nm argon laser. Images were analyzed and adapted with Zeiss LSM510 software and the program IrfanView Version 3.80 (<http://www.irfanview.de>).

Quantification of Gibberellins

The method used for extraction and quantification of endogenous gibberellins was based on the already established procedure of Lee et al. (1998). A 0.5 gram lyophilized sample was used for GA analysis each time. Gas chromatography (GC) (Hewlett-Packard 6890, 5973N Mass Selective Detector) with HA-1 capillary column (30 × 0.25 mm i.d., 0.25 μm film thickness) was used with oven temperature programmed for 1 min at 60°C, then a rise of 15°C min⁻¹ to 200°C, followed by 5°C min⁻¹ to 285 °C. Helium carrier gas was maintained at a head pressure of 30 kPa. The GC was directly interfaced to a Mass Selective Detector and source temperature of 280°C, an ionizing voltage of 70 eV and a dwell time of 100 ms. Full scan mode (the first trial) and three major ions of the supplemented [²H₂] gas internal standards (the second trial) and the endogenous gibberellins were monitored simultaneously (standard GAs were purchased from Prof. Lewis N. Mander, Australia National University, Canberra, Australia). The endogenous GA content was calculated from the peak area ratios. Retention time was determined by the hydrocarbon standards to calculate the KRI (Kovats Retention Indices) value (Kovats 1958)

Two-dimensional Polyacrylamide Gel Electrophoresis (2-D PAGE)

Protein extraction was performed by using 30-d-old wild type plants, *SEN1::AtGA2ox4* plants and GA3 treated *SEN1::AtGA2ox4* plants, respectively. In brief, LN2-frozen tissues were ground and mixed with 10 vol. of extraction buffer (7 M urea, 2 M thiourea, 4% (w/v) 3-[(3-cholamidopropyl) dimethylammonio]-1-propanesulfonate (CHAPS), 1% (w/v) dithiothreitol, 2% (v/v) pharnalyte, 1 mM benzamidine) for 30 min. with stirring, and then incubated at 100°C for 10 min. After centrifugation (15,000 rpm 60 min⁻¹), supernatant was used for 2-D PAGE. 2-D PAGE was performed as described previously (Rabilloud et al. 1998). Briefly, total protein extract was separated by using an IPG strip with a non-linear pH gradient of 4 to 10 (Genomine, Kyungbuk, Korea) for the first dimension, followed by SDS-PAGE

for the second dimension. Proteins were detected by alkaline silver staining (Rabilloud et al. 1998). Quantification of protein spots was carried out using PDQuest™ software (Bio-Rad, Hercules, CA, USA) and the quantity of protein in each spot was normalized against total valid spot intensity. For protein identification, protein spots were excised, digested with trypsin (Promega, Madison, WI, USA), mixed with α-cyano-4-hydroxycinnamic acid in 50% aqueous acetonitrile/0.1% trifluoroacetic acid, then subjected to MALDI-TOF analysis (Ettan MALDI-TOF, Amersham Biosciences, Piscataway, NJ) as described previously (Fernandez et al. 1998). The ProFound program (<http://prowl.rockefeller.edu/prowl-cgi/profound.exe>) was used to search the NCBI nr database for protein identification. The following parameters were used for the database search: trypsin as cleaving enzyme; a maximum of one missed cleavage; iodoacetamide (Cys) as a complete modification; methionine as a partial modification; monoisotopic masses; and a mass tolerance of 60.1 Da.

Acknowledgements

This work was supported by Basic Science Research Program through the National Research Foundation of Korea (NRF) (2011-0008840), a grant from the Korea Forest Service (S111213L080110), and Bio-industry Technology Development Program, Ministry of Agriculture, Food and Rural Affairs (112124-5), Korea.

Author's Contributions

DHL and JHK designed the experimental plan, analyzed the data and wrote the manuscript; ICL, KJK, DSK, HJN, ILL, SMK, HWJ, and PYL performed the experiments. All the authors agreed on the contents of the paper and post no conflicting interest.

Supporting Information

Table S1. Primers used in this study.

Fig. S1. Diagram of pSEN vector used in this study pSEN indicates SEN1 promoter and restriction enzyme sites in MCS are shown after pSEN.

References

- Appleford NE, Wilkinson MD, Ma Q, Evans DJ, Stone MC, Pearce SP, Powers SJ, Thomas SG, Jones HD, Phillips AL, Hedden P, Lenton JR (2007) Decreased shoot stature and grain alpha-amylase activity following ectopic expression of a gibberellin 2-oxidase gene in transgenic wheat. *J Exp Bot* 58:3213–3226
- Biemelt S, Tschiersch H, Sonnewald U (2004) Impact of altered gibberellin metabolism on biomass accumulation, lignin biosynthesis, and photosynthesis in transgenic tobacco plants. *Plant Physiol* 135:254–265
- Busov VB, Meilan R, Pearce DW, Ma C, Rood SB, Strauss SH (2003) Activation tagging of a dominant gibberellin catabolism gene (*GA 2-oxidase*) from poplar that regulates tree stature. *Plant Physiol* 132:1283–1291
- Cheng H, Qin L, Lee S, Fu X, Richards DE, Cao D, Luo D, Harberd NP, Peng J (2004) Gibberellin regulates Arabidopsis floral development via suppression of DELLA protein function.

- Development 131:1055–1064
- Chhun T, Aya K, Asano K, Yamamoto E, Morinaka Y, Watanabe M, Kitano H, Ashikari M, Matsuoka M, Ueguchi-Tanaka M (2007) Gibberellin regulates pollen viability and pollen tube growth in rice. *Plant Cell* 19:3876–3888
- Chung BC, Lee SY, Oh SA, Rhew TH, Nam HG, Lee CH (1997) The promoter activity of *sen1*, a senescence-associated gene of *Arabidopsis*, is repressed by sugars. *J Plant Physiol* 151:339–345
- Clough SJ, Bent AF (1998) Floral dip: a simplified method for *Agrobacterium*-mediated transformation of *Arabidopsis thaliana*. *Plant J* 16:735–43
- Curtis MD, Grossniklaus U (2003) A gateway cloning vector set for high-throughput functional analysis of genes in planta. *Plant Physiol* 133:462–469
- Dijkstra C, Adams E, Bhattacharya A, Page AF, Anthony P, Kourmpetli S, Power JB, Lowe KC, Thomas SG, Hedden P, Phillips AL, Davey MR (2008) Over-expression of a gibberellin 2-oxidase gene from *Phaseolus coccineus* L. enhances gibberellin inactivation and induces dwarfism in *Solanum* species. *Plant Cell Rep* 27:463–470
- El-Sharkawy I, El Kayal W, Prasath D, Fernandez H, Bouzayen M, Svircev AM, Jayasankar S (2012) Identification and genetic characterization of a gibberellin 2-oxidase gene that controls tree stature and reproductive growth in plum. *J Exp Bot* 63:1225–1239
- Fernandez J, Gharahdaghi F, Mische SM (1998) Routine identification of proteins from sodium dodecyl sulfate-polyacrylamide gel electrophoresis (SDS-PAGE) gels or polyvinyl difluoride membranes using matrix assisted laser desorption/ionization time-of-flight mass spectrometry (MALDI-TOF-MS). *Electrophoresis* 19:1036–1045
- Fleet CM, Sun TP (2005) A DELLAcate balance: the role of gibberellin in plant morphogenesis. *Curr Opin Plant Biol* 8:77–85
- Harberd NP, King KE, Carol P, Cowling RJ, Peng J, Richards DE (1998) Gibberellin: inhibitor of an inhibitor of...? *Bioessays* 20:1001–1008
- Hedden P (2003) The genes of the green revolution. *Trends Genet* 19:5–9
- Hedden P, Phillips AL (2000) Gibberellin metabolism: new insights revealed by the genes. *Trends Plant Sci* 5:523–530
- Hedden P, Thomas SG (2012) Gibberellin biosynthesis and its regulation. *Biochem J* 444:11–25
- Hisamatsu T, King RW (2008) The nature of floral signals in *Arabidopsis*. II. Roles for *FLOWERING LOCUS T* (FT) and gibberellin. *J Exp Bot* 59:3821–3829
- Hu J, Mitchum MG, Barnaby N, Ayele BT, Ogawa M, Nam E, Lai WC, Hanada A, Alonso JM, Ecker JR, Swain SM, Yamaguchi S, Kamiya Y, Sun TP (2008) Potential sites of bioactive gibberellin production during reproductive growth in *Arabidopsis*. *Plant Cell* 20:320–336
- Huang J, Tang D, Shen Y, Qin B, Hong L, You A, Li M, Wang X, Yu H, Gu M, Cheng Z (2010) Activation of gibberellin 2-oxidase 6 decreases active gibberellin levels and creates a dominant semi-dwarf phenotype in rice (*Oryza sativa* L.). *J Genet Genomics* 37:23–36
- Jasinski S, Piazza P, Craft J, Hay A, Woolley L, Rieu I, Phillips A, Hedden P, Tsiantis M (2005) KNOX action in *Arabidopsis* is mediated by coordinate regulation of cytokinin and gibberellin activities. *Curr Biol* 15:1560–1565
- Ko JH, Kim WC, Han KH (2009) Ectopic expression of MYB46 identifies transcriptional regulatory genes involved in secondary wall biosynthesis in *Arabidopsis*. *Plant J* 60:649–665
- Kovats E (1958) Gas chromatographische charakterisierung organischer Verbindungen. I. Retentions indices aliphatischer halogenide, alkohole, aldehyde und ketone. *Helv Chim Acta* 41:1915–1932
- Lee JJ, Foster KR, Morgan PW (1998). Photoperiod control of gibberellin levels and flowering in *Sorghum*. *Plant Physiol* 116:1003–1010
- Lester DR, Ross JJ, Smith JJ, Elliott RC, Reid JB (1999) Gibberellin 2-oxidation and the *SLN* gene of *Pisum sativum*. *Plant J* 19:65–73
- MacMillan J (2001) Occurrence of gibberellins in vascular plants, fungi, and bacteria. *J Plant Growth Regul* 20:387–442
- Martin DN, Proebsting WM, Hedden P (1999) The *SLENDER* gene of pea encodes a gibberellin 2-oxidase. *Plant Physiol* 121:775–781
- Mutasa-Gottgens E, Hedden P (2009) Gibberellin as a factor in floral regulatory networks. *J Exp Bot* 60:1979–1989
- Oh SA, Lee SY, Chung IK, Lee CH, Nam HG (1996) A senescence-associated gene of *Arabidopsis thaliana* is distinctively regulated during natural and artificially induced leaf senescence. *Plant Mol Biol* 30:739–754
- Olaszewski N, Sun TP, Gubler F (2002) Gibberellin signaling: biosynthesis, catabolism, and response pathways. *Plant Cell* 14 Suppl:S61–80
- Otani M, Meguro S, Gondaira H, Hayashi M, Saito M, Han DS, Inthima P, Supaibulwatana K, Mori S, Jikumaru Y, Kamiya Y, Li T, Niki T, Nishijima T, Koshioka M, Nakano M (2013) Overexpression of the gibberellin 2-oxidase gene from *Torenia fournieri* induces dwarf phenotypes in the liliaceous monocotyledon *Tricyrtis* sp. *J Plant Physiol* 170:1416–1423
- Peng J, Richards DE, Hartley NM, Murphy GP, Devos KM, Flintham JE, Beales J, Fish LJ, Worland AJ, Pelica F, Sudhakar D, Christou P, Snape JW, Gale MD, Harberd NP (1999) ‘Green revolution’ genes encode mutant gibberellin response modulators. *Nature* 400:256–261
- Rabilloud T, Kieffer S, Procaccio V, Louwagie M, Courchesne PL, Patterson SD, Martinez P, Garin J, Lunardi J (1998) Two-dimensional electrophoresis of human placental mitochondria and protein identification by mass spectrometry: toward a human mitochondrial proteome. *Electrophoresis* 19:1006–1014
- Radi A, Lange T, Niki T, Koshioka M, Lange MJ (2006) Ectopic expression of pumpkin gibberellin oxidases alters gibberellin biosynthesis and development of transgenic *Arabidopsis* plants. *Plant Physiol* 140:528–536
- Rieu I, Eriksson S, Powers SJ, Gong F, Griffiths J, Woolley L, Benlloch R, Nilsson O, Thomas SG, Hedden P, Phillips AL (2008a) Genetic analysis reveals that C19-GA 2-oxidation is a major gibberellin inactivation pathway in *Arabidopsis*. *Plant Cell* 20:2420–2436
- Rieu I, Ruiz-Rivero O, Fernandez-Garcia N, Griffiths J, Powers SJ, Gong F, Linhartova T, Eriksson S, Nilsson O, Thomas SG, Phillips AL, Hedden P (2008b) The gibberellin biosynthetic genes *AtGA20ox1* and *AtGA20ox2* act, partially redundantly, to promote growth and development throughout the *Arabidopsis* life cycle. *Plant J* 53:488–504
- Sakamoto T, Kobayashi M, Itoh H, Tagiri A, Kayano T, Tanaka H, Iwahori S, Matsuoka M (2001) Expression of a gibberellin 2-oxidase gene around the shoot apex is related to phase transition in rice. *Plant Physiol* 125:1508–1516
- Sakamoto T, Morinaka Y, Ishiyama K, Kobayashi M, Itoh H, Kayano T, Iwahori S, Matsuoka M, Tanaka H (2003) Genetic manipulation of gibberellin metabolism in transgenic rice. *Nat Biotechnol* 21:909–913
- Schomburg FM, Bizzell CM, Lee DJ, Zeevaert JA, Amasino RM (2003) Overexpression of a novel class of gibberellin 2-oxidases decreases gibberellin levels and creates dwarf plants. *Plant Cell* 15:151–163
- Silverstone AL, Jung HS, Dill A, Kawaide H, Kamiya Y, Sun TP (2001) Repressing a repressor: gibberellin-induced rapid reduction of the RGA protein in *Arabidopsis*. *Plant Cell* 13:1555–1566

- Singh DP, Jermakow AM, Swain SM (2002) Gibberellins are required for seed development and pollen tube growth in *Arabidopsis*. *Plant Cell* 14:3133–3147
- Solfanelli C, Ceron F, Paolicchi F, Giorgetti L, Geri C, Ceccarelli N, Kamiya Y, Picciarelli P (2005) Expression of two genes encoding gibberellin 2- and 3-oxidases in developing seeds of *Phaseolus coccineus*. *Plant Cell Physiol* 46:1116–1124
- Sun TP, Kamiya Y (1994) The *Arabidopsis* *GAI* locus encodes the cyclase ent-kaurene synthetase A of gibberellin biosynthesis. *Plant Cell* 6:1509–1518
- Thomas SG, Phillips AL, Hedden P (1999) Molecular cloning and functional expression of gibberellin 2-oxidases, multifunctional enzymes involved in gibberellin deactivation. *Proc Natl Acad Sci USA* 96:4698–4703
- Ueguchi-Tanaka M, Ashikari M, Nakajima M, Itoh H, Katoh E, Kobayashi M, Chow TY, Hsing YI, Kitano H, Yamaguchi I, Matsuoka M (2005) *GIBBERELLIN INSENSITIVE DWARF1* encodes a soluble receptor for gibberellin. *Nature* 437:693–698
- Yamaguchi S (2008) Gibberellin metabolism and its regulation. *Annu Rev Plant Biol* 59:225–251
- Zhou B, Peng D, Lin J, Huang X, Peng W, He R, Guo M, Tang D, Zhao X, Liu X (2011) Heterologous expression of a gibberellin 2-oxidase gene from *Arabidopsis thaliana* enhanced the photosynthesis capacity in *Brassica napus* L. *J Plant Biol* 54:23–32